Chapter 7
On Molecular Dynamics of the Diamond D_5 Substructures

Beata Szefler

Abstract Diamond D_5 is a hyperdiamond, with the rings being mostly pentagonal and built up on the frame of *mtn* structure, appearing in type II clathrate hydrates. The centrohexaquinane C_{17} was proposed as the seed of D_5 (Diudea, Studia Univ Babes-Bolyai Chemia, 55(4):11–17, 2010a; Diudea, Nanomolecules and nanostructures – polynomials and indices. University of Kragujevac, Kragujevac, 2010b). In this chapter, we present some results on molecular dynamics (MD) of four structures based on C_{17} skeleton, as all-carbon or partly oxygenated derivatives. The results are discussed in terms of structural stability as given by DFT calculations as well as by the stable fluctuations of root-mean-square deviations (*RMSD*) and total, potential, and kinetic energies provided by MD calculations. Within D_5, several other substructures are discussed in this chapter. The structural stability of such intermediates/fragments appearing in the construction/destruction of D_5 net is also discussed in terms of molecular dynamics simulation. The calculations herein discussed have been done using an empirical many-body potential energy function for hydrocarbons. It has been found that, at normal temperature, the hexagonal hyper-rings are more stable, while at higher temperature, the pentagonal ones are relatively stronger against the heat treatment.

7.1 Introduction

In the nano-era, a period starting with the discovery of $C_{60,}$ in 1985, the carbon allotropes played a dominant role. Among the carbon structures, fullerenes (zero dimensional), nanotubes (one dimensional), graphene (two dimensional), diamond,

B. Szefler (✉)
Department of Physical Chemistry, Collegium Medicum, Nicolaus Copernicus University, Kurpińskiego 5, 85-950 Bydgoszcz, Poland
e-mail: beata.szefler@cm.umk.pl

M.V. Diudea and C.L. Nagy (eds.), *Diamond and Related Nanostructures*, Carbon Materials: Chemistry and Physics 6, DOI 10.1007/978-94-007-6371-5_7,

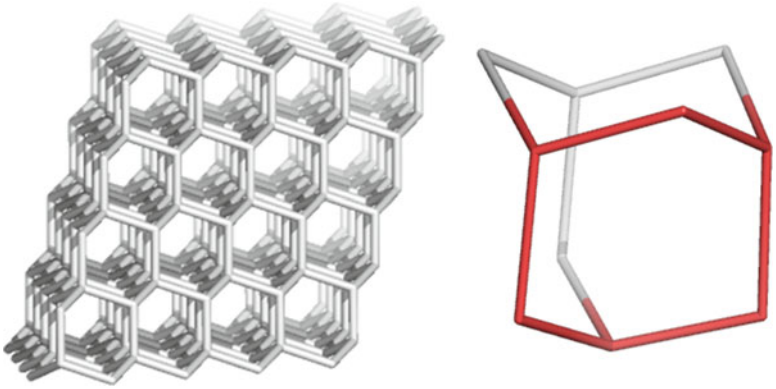

Fig. 7.1 Diamond D_6 (*left*) and its repeating unit, adamantane (*right*)

and spongy carbon (three dimensional) were the most studied (Diudea 2005, 2010a; Diudea and Nagy 2007), both from theoretical reasons and applications perspective.

Diamond D_6, the beautiful classical diamond, with all-hexagonal rings of sp^3 carbon atoms (Fig. 7.1), crystallized in the face-centered cubic *fcc* network (space group *Fd*-3*m*), has kept its leading interest among the carbon allotropes, in spite of the "nano" varieties (Decarli and Jamieson 1961; Aleksenskiĭ et al. 1997; Osawa 2007, 2008; Williams et al. 2007; Dubrovinskaia et al. 2006). Its aesthetical appeal and mechanical characteristics are of great importance in jewelry and industry. Synthetic diamonds are currently produced by a variety of methods, including high pressure-high temperature (HPHT), chemical vapor deposition (CVD), and ultrasound cavitation (Khachatryan et al. 2008).

However, the diamond D_6 is not unique: a hexagonal network called lonsdaleite (space group $P6_3/mmc$) (Frondel and Marvin 1967) was discovered in a meteorite in the Canyon Diablo, Arizona, in 1967. Several diamond-like networks have also been proposed (Diudea et al. 2010; Hyde et al. 2008).

In a previous study, Diudea and Ilić (2011) described some multi-tori (i.e., structures showing multiple hollows (Diudea and Petitjean 2008)); one of them is illustrated in Fig. 7.2, left.

The reduced graph of this multi-torus provided the structure for the seed of diamond D_5: C_{17} (Fig. 7.2, right) consisting of a tetravalent atom surrounded by six pentagons, the maximum possible number of pentagons around an sp^3 carbon atom. According to the chemical nomenclature, C_{17} is a centrohexaquinane, a class of structures previously studied by Gund and Gund (1981), Paquette and Vazeux (1981), and more recently by Kuck (1984, 2006) and Kuck et al. (1995).

Diamond D_5 is the name given by Diudea to diamondoids consisting mostly of pentagonal rings (Diudea 2010a, b; Diudea and Ilić 2011). D_5 is a hyperdiamond built up in the frame of the trinodal *mtn* structure, while its seed is eventually the centrohexaquinane C_{17}. However, D_5 belongs to the family of Clathrates with the point symbol net {5^5.6}12{5^6}5 and $2[5^{12}] + [5^{12} \times 6^4]$ tiling and belongs to the

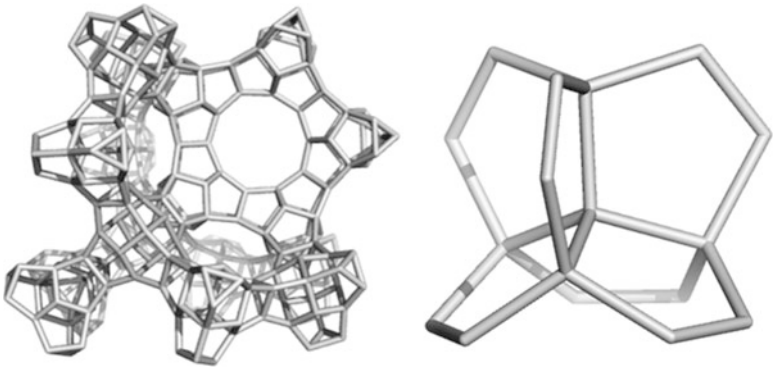

Fig. 7.2 A multi-torus (*left*) and its reduced graph C_{17} (*right*), the seed of diamond D_5

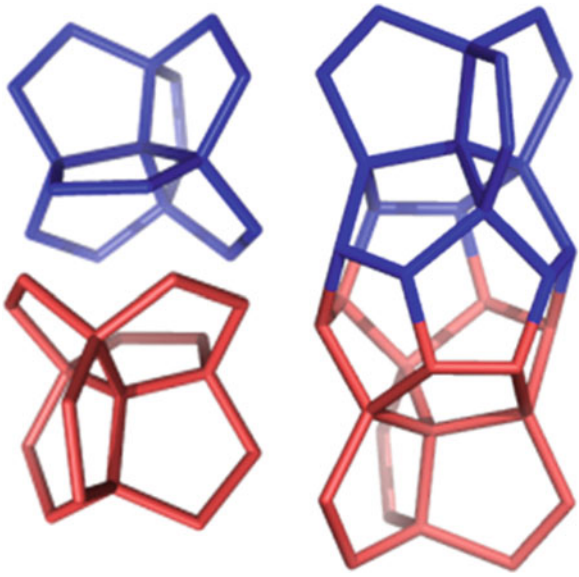

Fig. 7.3 A joint of two C17 units (*left*) to give a dimer C34 (*right*), the repeat unit (in crystallographic terms) of the diamond D_5 network

space group *Fd*3*m* (Delgado-Friedrichs et al. 2005). It is precisely type II clathrate, also called C_{34} (Blasé et al. 2010), of which Si_{34}-analogue was already synthesized.

C_{17} can dimerize to $2 \times C_{17} = C_{34}$ (Fig. 7.3), the repeating unit, in crystallographic terms, of the diamond D_5 network. Thus, D_5 (Fig. 7.4) and *fcc*-C_{34} are herein synonyms (Fig. 7.5).

In a chemist's view, the building of D_5 network may start with the seed C_{17} and continue with some intermediates, the adamantane- and diamantane-like ones included (Figs. 7.6, 7.7, and 7.8). The structure ada_20_158 (Fig. 7.7, left) corresponds to adamantane (Fig. 7.5, left) in the classical diamond D_6. In crystallochemical terms, an adamantane-like structure, as ada_20_158, is the

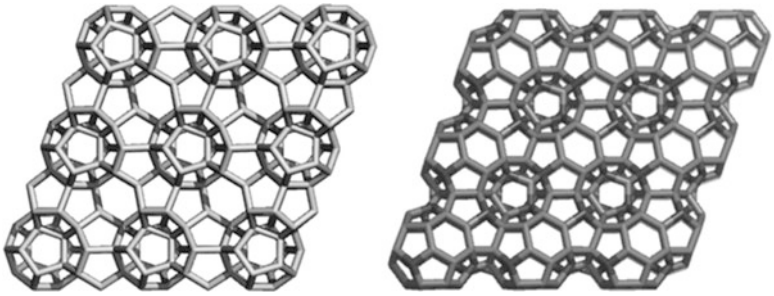

Fig. 7.4 Diamond D_5_20_860 net (*left*) and D_5_28_1022 co-net (*right*)

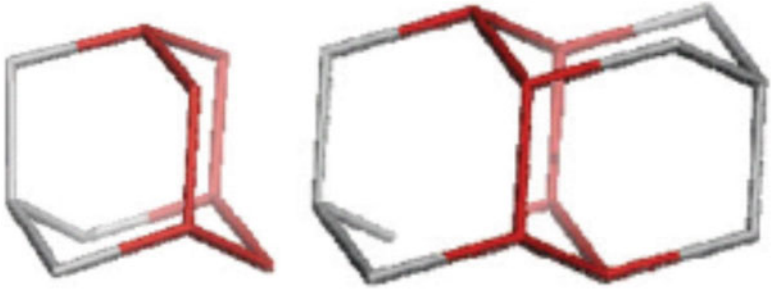

Fig. 7.5 Diamond D_6: adamantane (*left*), diamantane (*right*)

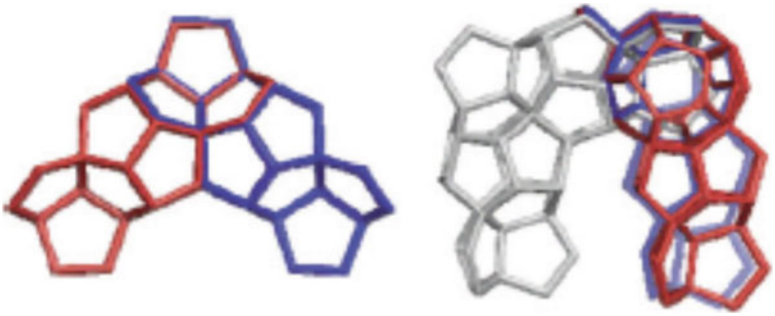

Fig. 7.6 Intermediate structures originating in C_{34} unit: C_{51} (*left*) and $3 \times C_{51}$ (*right*)

monomer which will probably condense to form the D_5 network (Fig. 7.4). The ada-like structure, starting from C_{28} can be seen in Fig. 7.7, right. Diamantane-like units can also be modeled, as in Fig. 7.8 (compare with the diamantane, Fig. 7.5, right). In fact, there is one and the same triple periodic D_5 network, built up basically from C_{20} and having as hollows the fullerene C_{28}. The co-net D_5_28 cannot be derived from C_{28} alone since the hollows of such a net consist of C_{57} units (a C_{20}-based

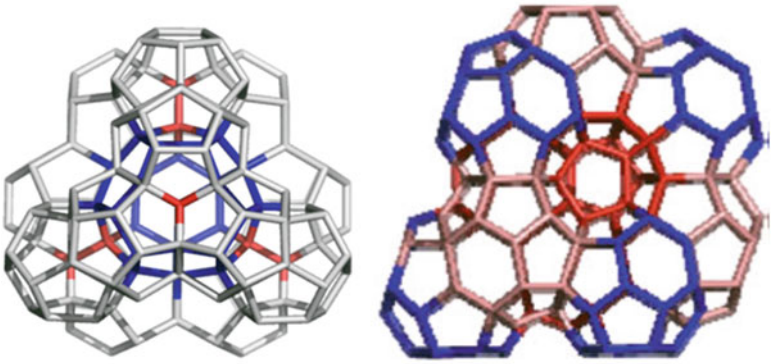

Fig. 7.7 Adamantane-like structures: ada_20_158 (*left*) and ada_28_213 (*right*)

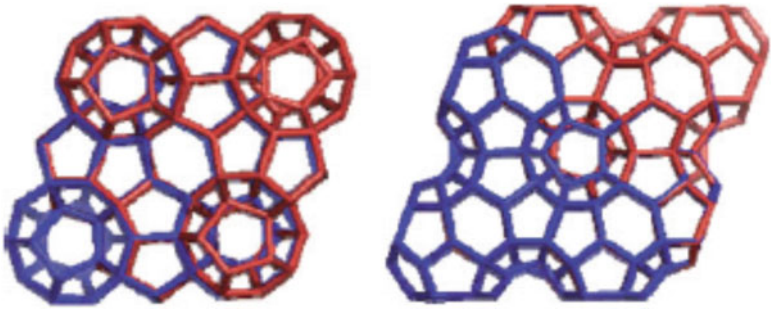

Fig. 7.8 Diamantane-like structures: dia_20_226 net (*left*) and dia_28_292 co-net (*right*)

structure, see above) or higher tetrahedral arrays of C_{20}, thus needing extra C atoms per ada-unit. It is worthy to note the stabilizing effect of the wings in case of C_{34} (Fig. 7.3, right) in comparison to C_{20}.

Remark the efforts made by a series of bright scientists (Prinzbach et al. 2006; Paquette et al. 1981; Saito and Miyamoto 2001; Eaton 1979) to reach the dodecahedral cage C_{20}, either as fullerene or hydrogenated species. Also remark the endeavor to synthesize the centrohexaquinane C_{17}, both as oxygen-containing heterocycle (Simmons and Maggio 1981; Paquette and Vazeux 1981) or all-carbon structure (Gestmann et al. 2006; Kuck 2006). Thus, the hyperdiamond D_5_20/28 mainly consists of sp^3 carbon atoms building ada-type repeating units (including C_{28} as hollows). The ratio C-sp^3/C-total trends to one in a large enough network. As the content of pentagons R[5] (Aleksenskiĭ et al. 1997; Williams et al. 2007) per total rings trend to 90 %, this network was named the diamond D_5 (Diudea 2010a, b).

In the above symbols, "20" refers to C_{20} and "28" refers to C_{28}, while the last number counts the carbon atoms in structures.

7.2 Method

In a study of structural stability, performed by Szefler and Diudea (2012), ab initio calculations and molecular dynamics have been used. The four structures (Figs. 7.9 and 7.12) based on C_{17} skeleton, as all-carbon or partly oxygenated derivatives, were optimized at the Hartree-Fock (HF) (HF/6-31G**) and DFT (B3LYP/6-311+G**) levels of theory and submitted to molecular dynamics (MD) procedure. All calculations were performed in gas phase by Gaussian 09 (Gaussian 09 software package 2009) while MD calculations were done in vacuum, using Amber 10.0 software (Case et al. 2005). The single-point energy minima obtained for the investigated structures are shown in Table 7.1. Before MD, the atomic charges were calculated according to Merz-Kollmann scheme via the RESP (Wang et al. 2000) procedure, at HF/6-31G** level. The AMBER force field (Wang et al. 2004) was used for dynamic trajectory generation. There were several steps of molecular dynamics. After stabilization of energies and RMSD values during run, the actual molecular dynamics were performed, in a cascade way. Each tested system was heated by 20 ps while MD simulations were 100 ns long. The visualizations were prepared in the GaussView program. After MD run, the values of RMSD and energies of analyzed structures were recorded: total energy (E_{tot}), kinetic energy (E_{kin}), and potential energy (E_{pot}). In the analysis, averaged values of all generated points of energies and values of RMSD in every 1 ps of MD were used.

The stability of 12 other substructures was investigated by Kyani and Diudea (2012) by performing a molecular dynamics (MD) computer simulation, using an empirical many-body adaptive intermolecular reactive empirical bond-order (AIREBO) potential energy function. All the diamond D_5 substructures are fully

Fig. 7.9 C_{17}_hexaquinane trioxo derivatives: Paquette P_1 (*left*) and Diudea, D_1 (*middle*) and D_2 (*right*)

Table 7.1 The single-point energies of the optimized structures at DFT (B3LYP/6-311+G**) level of theory

B3LYP	C_{17}	D_1	D_2	P_1
B3LYP (a.u)	−655.058	−766.491	−766.480	−766.479
B3LYP_Gap (eV)	5.868	6.461	6.264	6.274

hydrogenated ones. The studied structures were optimized at the semiempirical PM3 level of theory and then submitted to the MD simulation procedure. Canonical ensemble molecular dynamics was used for this simulation. Within this ensemble, the number of atoms N, the volume V, and the temperature T are considered constants while velocities are scaled with respect to T, ensuring that the total kinetic energy, and hence the temperature, is constant (isokinetic MD). The initial velocities follow the Maxwell distribution. The AIREBO potential energy function (PEF) developed for hydrocarbons (Stuart et al. 2000), as provided by LAMMPS software (Plimpton 1995), was used to investigate the stability of nanostructures at increasing temperatures. This parameterized potential adds Lennard-Jones and torsional contributions to the many-body REBO potential (Brenner 2000; Brenner et al. 2000). It is similar to a pairwise dispersion-repulsion potential, while adding a bond-order function modulates the dispersion term and incorporates the influence of the local atomic environment. Through this interaction, individual atoms are not constrained to remain attached to specific neighbors, or to maintain a particular hybridization state or coordination number. Thus, at every stage of the simulation, the forming and breaking of the bonds is possible. This potential is derived from ab initio calculations, and therefore, it is well adapted to classical molecular simulations of systems containing a large number of atoms such as carbon nanostructures. The equations of particle motion were solved using the Verlet algorithm (Verlet 1967, 1968), and the temperature was gradually increased by 100 K at each run. One time step was taken to be 10–16 s and at each run a relaxation with 5,000 time steps was performed. The root-mean-square deviation (RMSD) of the atoms was used as criterion for examining the stability of the simulated structures.

7.3 Results and Discussion

Stability evaluation was performed on four hypothetical seeds of D_5, the all-carbon structure C_{17} (Fig. 7.2, right) and three trioxa derivatives of C_{17}. The isomer in Fig. 7.9, left, was synthesized by Paquette and Vazeux (1981) and is hereafter denoted as P_1. Other two structures, denoted as D_1 and D_2 (Fig. 7.9, middle and right), were proposed (Szefler and Diudea 2012), as possibly appearing in rearrangements of the Paquette's P_1 structure. The last two structures would be the appropriate ones in the next step of dimerization to C_{34}, in fact the repeating unit of D_5 (Blasé et al. 2010).

The stability of molecules was evaluated both in static and dynamic temperature conditions. The isomer D_1 seems the most stable among all studied structures, as given by optimization in gas phase at DFT level (Table 7.1). In a decreasing order of stability, it follows P_1 and D_2. However, at MD treatment, the all-carbon C_{17} appears the most stable, even at DFT level is the last one. This is probably because the C–C bond is more stable at temperature variations (see Fig. 7.12, below).

In MD, C_{17} keeps its structure up to about 1,800 K, while its destruction starts at 2,000 K (Tables 7.2 and 7.4, Figs. 7.10 and 7.11). Kuck has reported a

Table 7.2 The average total energy (E_{tot}) values estimated, by MD, on geometries in the gas phase

C_{17}							
TEMP (K)	300	600	900	1,200	1,400	1,600	1,800
E_{tot} (kcal/mol)	127.405	180.379	233.358	286.460	322.227	357.665	393.123
δ	5.789	11.585	17.373	23.121	27.070	30.932	34.938
D_1							
TEMP (K)	300	600	900	1,200	1,400	1,600	
E_{tot} (kcal/mol)	144.996	197.907	250.689	303.114	337.947	373.136	
δ	5.782	11.593	17.273	23.106	26.739	30.745	
D2							
TEMP (K)	300	600	900				
E_{tot} (kcal/mol)	116.45	169.266	222.049				
δ	5.783	11.542	17.363				
P1							
TEMP (K)	300	600	900	1,200	1,400	1,600	
E_{tot} (kcal/mol)	142.574	195.448	247.889	300.329	335.524	370.602	
δ	5.798	11.535	17.300	23.076	26.931	30.678	

The averaged values were calculated on all the generated points of energies in every 1 ps of molecular dynamics
Symbol δ means the standard deviation

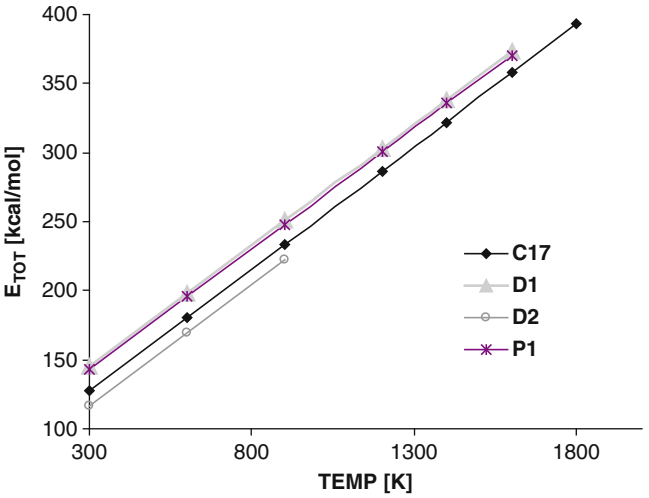

Fig. 7.10 The plot of total energy (E_{tot}) versus temperature (TEMP)

centrohexaindane as the most symmetric structure in this series but also a benzo-centrohexaquinane (Kuck et al. 1995; Kuck 2006) as the last step structure in the synthesis of a nonplanar 3D structure, designed according to mathematical rules. However, in the synthesis of centrohexaquinane derivatives, C_{17} remained yet elusive.

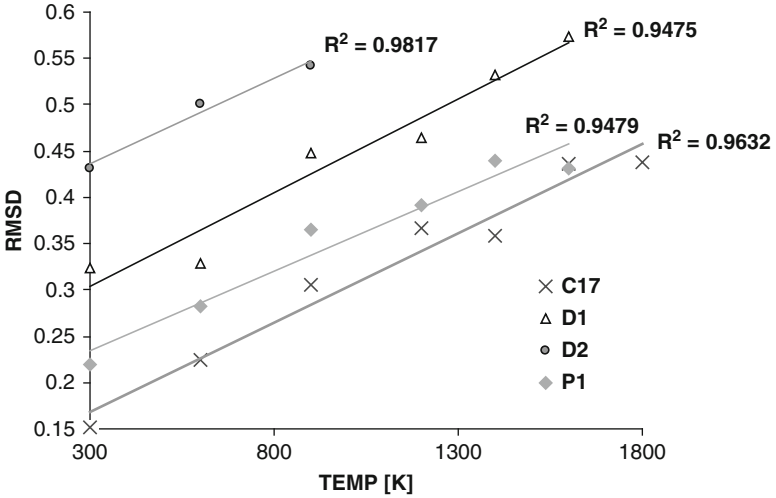

Fig. 7.11 The plot of RMSD versus temperature (TEMP)

Very close to C_{17} behaves the oxygen-containing isomer D_1, as expected from its highest stability at DFT level.

Despite, in molecular dynamics, a very long time (100ns) was leaded, it is believed that prolonged annealing at 1,800 K for both P_1 and D_1 isomers finally resulted in the destruction of these molecules. Thus, P_1 and D_1 isomers behave similarly in MD conditions. The isomer D_2 was the least stable one, as the largest RMSD values were recorded for this isomer.

According to molecular dynamics, it is clear that increasing the temperature resulted in higher values of energy and RMSD of all the analyzed structures, with high values of correlation. The plots of E_{tot} versus temperature for all tested systems are given in Fig. 7.10, while for RMSD, the plots are given in Fig. 7.11. As expected, the correlations in the RMSD plot are a little lower than those for E_{tot}. The MD calculations, listed in Tables 7.2, 7.3, and 7.4, show the following.

As can be seen from Tables 7.2 and 7.3, the values of standard deviations of the averaged values of E_{tot} are closely correlated with the values of temperature, in the range the molecular dynamics simulations were done. The values of these standard deviations at a given temperature are similar for all four studied structures, due to their structural relatedness. The smallest values of the RMS deviation are observed for C_{17}, with the lowest values of standard deviation (δ) at all the studied values of temperature (Table 7.4).

In the case of P_1, one can see a similar behavior but somewhat with larger values of RMSD, compared to the all-carbon structure C_{17} (Table 7.4). It confirms the structural stability of the above structures. The largest values of the RMS deviation were recorded for D_2 isomer (Table 7.4 and Fig. 7.11). Visualization of the structural changes (first step destruction, the right column) is presented in Fig. 7.12.

Table 7.3 The values of standard deviations of E_{tot} at a given temperature (see the center of each slide) for the four investigated structures

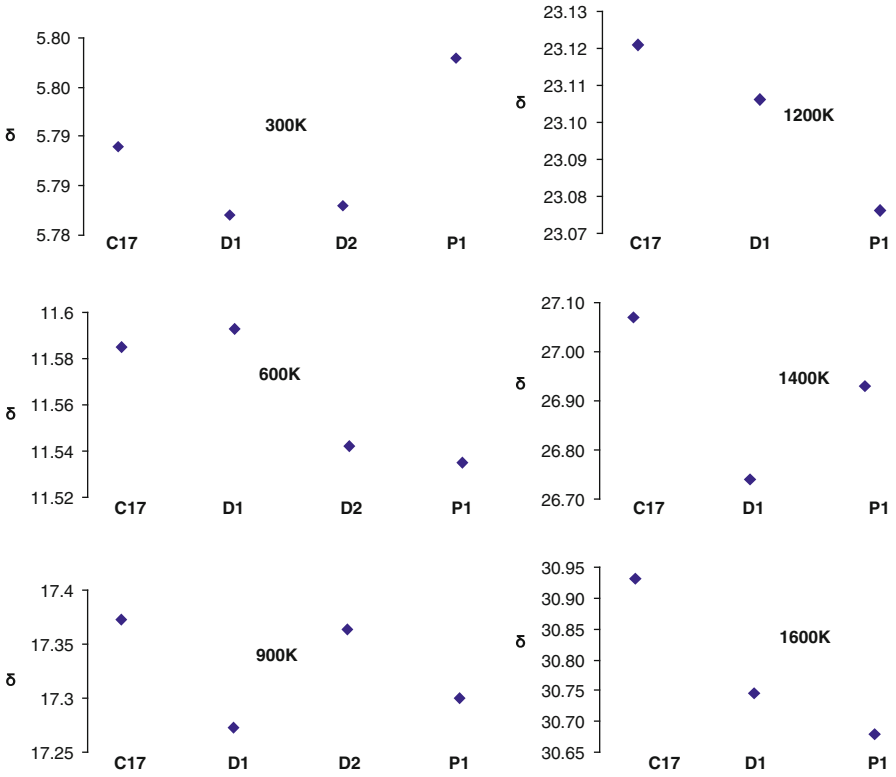

When discussing about diamonds, we consider structures consisting mostly of sp^3 hybridized carbon atom. The molecular dynamic with formulation and parametrization intended for carbon system is REBO (Tersoff 1988a, b; Abell 1985). The Tersoff's and Brenner's (Brenner 1990, 1992) models could describe single-, double-, and triple-bond energies in carbon structures such as hydrocarbons and diamonds, where extended Tersoff's potential function is extended to radical and conjugated hydrocarbon bonds by introducing two additional terms into the bond-order function. Compared to the classical first-principle and semiempirical approaches, the REBO model is less time-consuming. In recent years, the REBO model has been widely used in studies concerning mechanical and thermal properties of carbon nanotubes (Ruoff et al. 2003; Rafii-Tabar 2004).

Molecular dynamic MD calculations using the REBO model were performed by Kyani and Diudea (2012) on the structures listed in Figs. 7.13 and 7.14. The last number in the symbol of structures refers to the number of carbon atoms.

Table 7.4 The averaged RMSD values estimated by molecular dynamics (MD) on the geometries in the gas phase

C_{17}							
TEMP (K)	300	600	900	1,200	1,400	1,600	1,800
RMSD	0.151	0.224	0.305	0.366	0.358	0.437	0.438
δ	0.024	0.032	0.045	0.056	0.054	0.054	0.062
D_1							
TEMP (K)	300	600	900	1,200	1,400	1,600	
RMSD	0.324	0.328	0.448	0.465	0.532	0.574	
δ	0.134	0.088	0.079	0.086	0.091	0.118	
D_2							
TEMP (K)	300	600	900				
RMSD	0.432	0.500	0.542				
δ	0.257	0.245	0.208				
P_1							
TEMP (K)	300	600	900	1,200	1,400	1,600	
RMSD	0.220	0.283	0.365	0.392	0.440	0.431	
δ	0.062	0.069	0.092	0.070	0.093	0.070	

The averaged values were calculated on all the generated points of RMSD in every 1 ps of MD
Symbol δ represents the standard deviation

The main reason for doing calculations on hydrogenated species, although the fragments can appear as non-hydrogenated ones, is the sp^3 hybridization of carbon atoms in the diamond structures. Thus, the four-valence state is preserved.

PM3 calculations show the hexagonal hyper-rings more stable than the pentagonal ones, either with a hollow or filled one as in case of lens-like structures (Table 7.5, entries 5, 6 and 10). There is one exception; the empty hexagon of C_{28} fullerenes (entry 9) is less stable than the corresponding empty pentagon (entry 7). The hexagonal filled ring structures are more stable than the empty ones, except the empty hexagon $20^6\_H_{60}$ (entry 5), made from C_{20}, which seems to be the most stable, as isolated structure, herein discussed. Similarly, $C_{20}H_{20}$ (entry 1) is the stabilized form of the most reactive/unstable fullerene C_{20}. The stabilizing effect of ring filling is a reminiscence of the infinite crystal lattice, whose substructures are $20^6\_28^2H_{68}$ (diamond D_5 net) and $28^6\_20^2H_{92}$ (lonsdaleite L_5 net).

As in studies of the stability of hypothetical seeds of the diamond D_5 by using Amber 10.0 for MD, also here we could see that with increasing temperature, the energy of the systems increases, what would be expected. The total energy versus temperature for three of the considered systems is illustrated in (Fig. 7.15).

MD simulations on increasing temperature evolution show that the studied structures are stable up to 2,000 K, for the C_{20}-based structures (Fig. 7.13), and up to 1,500–2,000 K, for the C_{28}-based structures (Fig. 7.14). The three numbers at the figure bottom represent temperatures, in K degree, for: geometry modifications, topology changes, and major destruction of the structure. Where there are only two data, the topological changes were not observed.

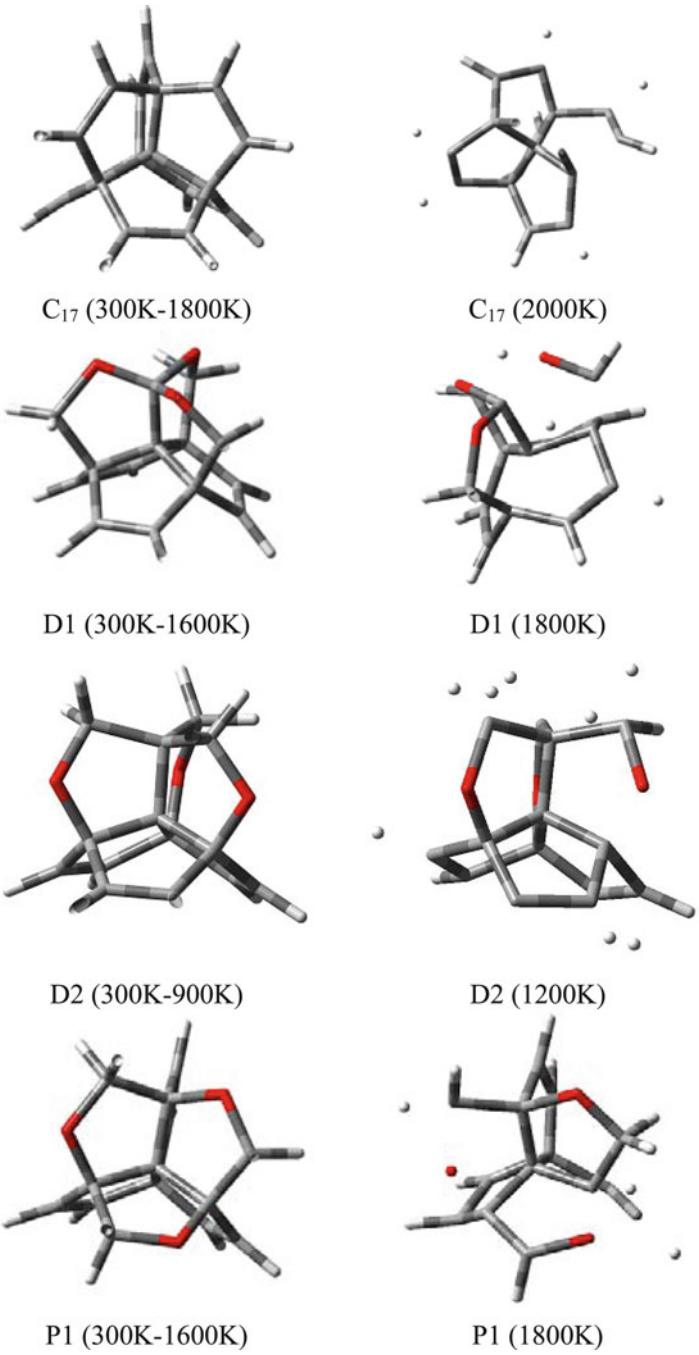

Fig. 7.12 The structure of the tested hypothetical seeds of the diamond D_5 during molecular dynamics

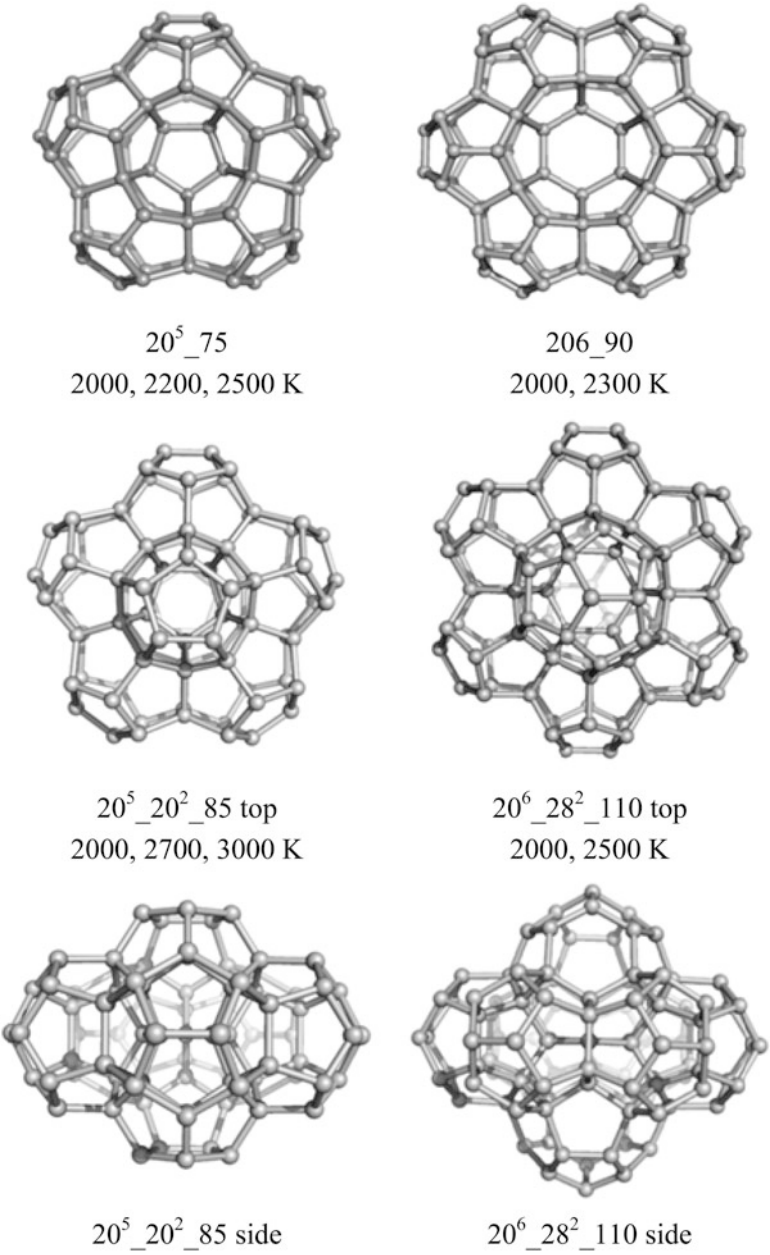

Fig. 7.13 C_{20}-based structures; $20^6\_28^2\_110$ a substructure of $D_5\_20/28$ (Reproduced from Central European Journal of Chemistry 2012, 10(4), 1028–1033)

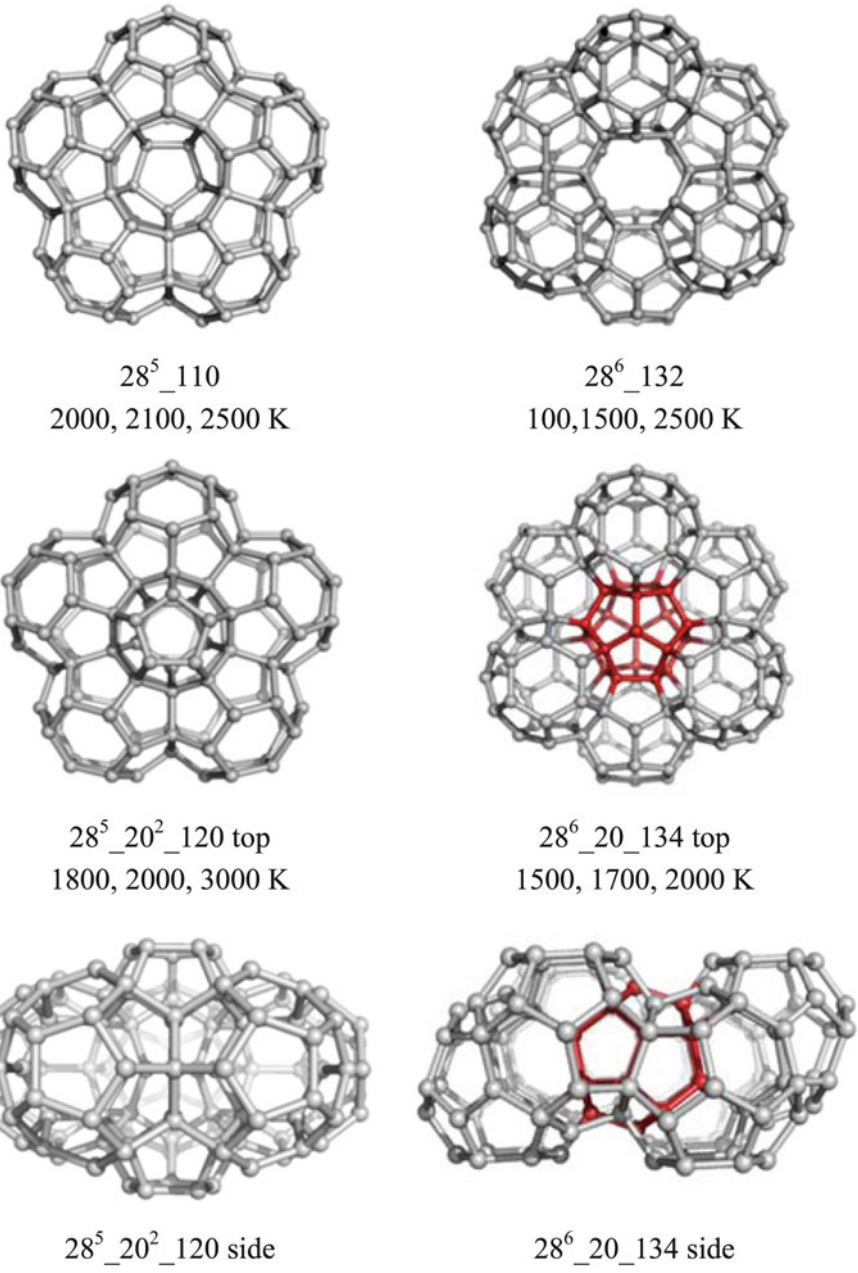

Fig. 7.14 C_{28}-based structures; 286_20_134 a substructure of L5_28/20. The *red* lines show the core substructure, that is C_{20} the smallest fullerene (Reproduced from Central European Journal of Chemistry 2012, 10(4), 1028–1033)

Table 7.5 PM3 energies calculated on fully hydrogenated species

	Structure	Total energy (a.u.)	Gap (eV)
1	$C_{20}H_{20}$	−0.0620	13.905
2	$C_{28}H_{28}$	−0.0035	13.769
3	$20^5\_H_{50}$	0.0045	12.953
4	$20^5\_20^2H_{50}$	0.0432	12.898
5	$20^6\_H_{60}$	−0.1215	13.198
6	$20^6\_28^2H_{68}$	−0.0167	13.061
7	$28^5\_H_{80}$	0.1564	13.034
8	$28^5\_20^2H_{80}$	0.1648	13.061
9	$28^6\_H_{60}$	0.3432	12.490
10	$28^6\_20^2H_{92}$	0.1353	13.034

Reproduced from Central European Journal of Chemistry 2012, 10(4), 1028–1033

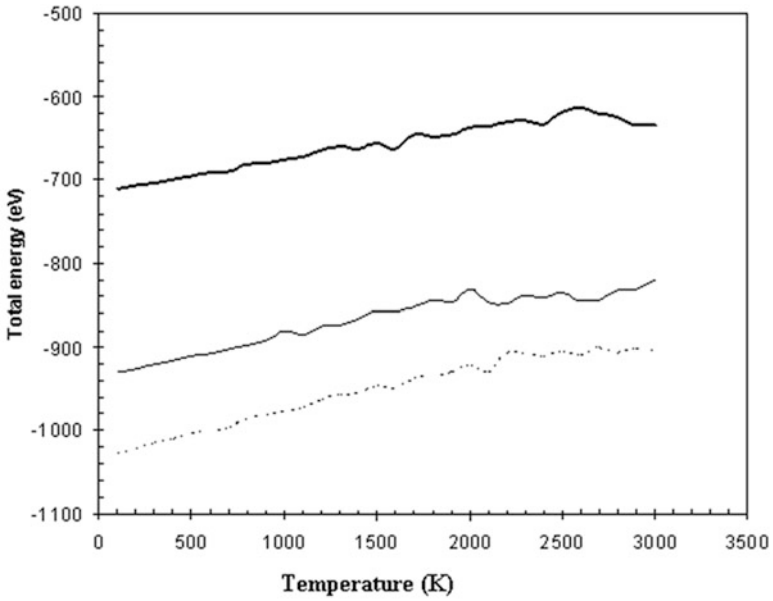

Fig. 7.15 Total energy versus temperature of some of the diamond D_5 substructures: $20^5\_20^2H_{50}$ (*solid line*, Table 7.5, entry 4), $20^6\_28^2H_{68}$ (*simple line*, Table 7.5, entry 6), and $28^5\_20^2H_{80}$ (*dotted line*, Table 7.5, entry 8) (Reproduced from Central European Journal of Chemistry 2012, 10(4), 1028–1033)

The structures in Fig. 7.16 show elongated bonds (i.e., broken bonds, marked by orange color) at temperatures above 2,000 K. Question about structure preserving must be addressed when more than one broken bond will appear (see the bottom row, Fig. 7.16). Above 2,500 K, the complete destruction is expected for all the three structures shown in Fig. 7.16; for two structures (those with only two temperatures on their bottom) the topological changes were not observed. In case of the basic fullerenes, the data are: $C_{20}H_{20}$, 2,700 and 3,000 K, and $C_{28}H_{28}$, 2,500, 2,600,

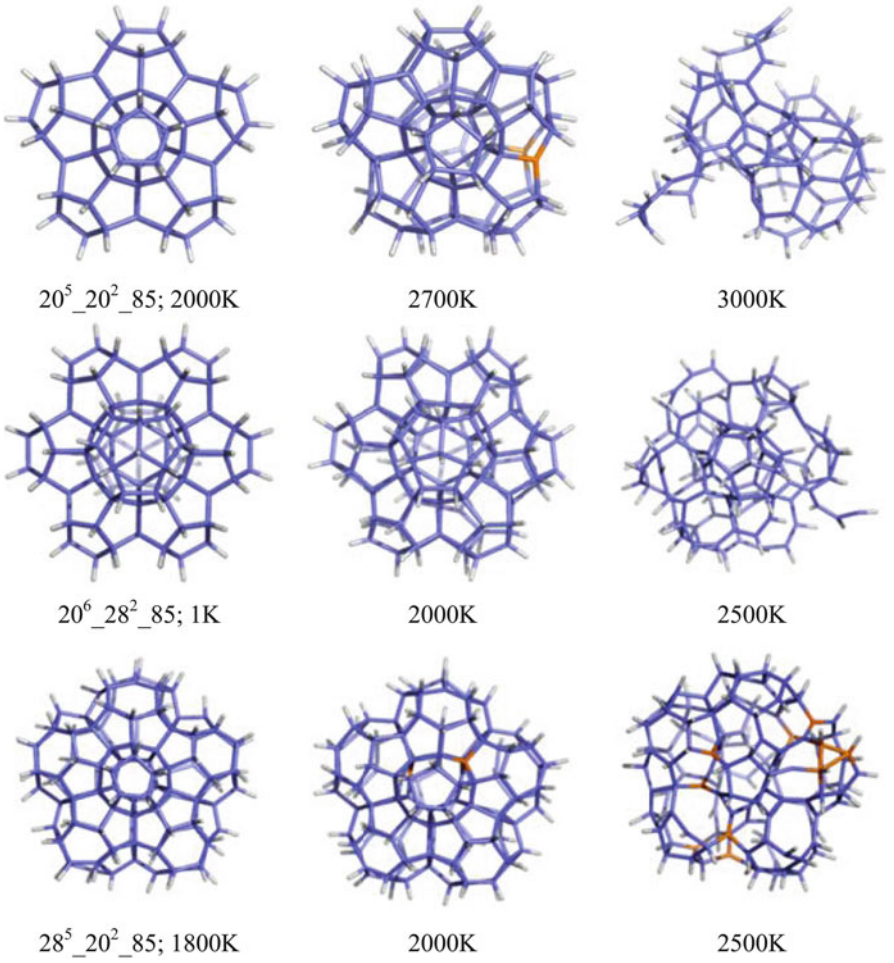

Fig. 7.16 Relaxed structures of $20^5\_20^2\_85$, $20^6\_28^2\_85$ and $28^5\_20^2\_85$ at various temperatures. The *orange* colors mark the broken/formed bonds (Reproduced from Central European Journal of Chemistry 2012, 10(4), 1028–1033)

and 3,000 K. Among the frequent topological changes, the most important is the expansion of two pentagons sharing an edge to octagon and also the apparition of trigons, squares, or larger rings before the structure dramatically decomposes. It is obvious that the structural changes will affect the energetics of the system.

The MD data agree with the PM3 data; in fact, the C_{20}-based structures are more stable than the C_{28}-ones, which corresponds to the higher stability of diamond D_5 compared to lonsdaleite L_5 (Aste and Weaire 2008). At higher temperature, the five-fold hyper-rings seem to be more stable, at least in the isolated fragments (see Figs. 8.13 and 8.14). Remind that such fragments can appear either in synthesis of D_5

or in its destruction, their knowledge thus being of real interest. It is important to know the limit temperature, e.g., in the annealing process of repeating unit C_{34} in the possible synthesis of D_5. Conversely, in the analysis of such diamondoids, the possible fragments appearing in the destruction of their lattice must be known.

7.4 Conclusions

In this chapter, structural stability of four seeds of the diamond D_5 and several substructures/fragments related to the D_5 diamond were investigated. In the first case, it was evaluated both in static and dynamic temperature conditions by molecular dynamics (MD). During MD, the all-carbon C_{17} appeared the most resistant to changes in temperature. Structural and energetic stability of the other three seeds of D_5 vary both with the values of temperature and evolution time in molecular dynamics and the arrangement of oxygen atoms in the molecules. Among all the studied structures, the D_2 isomer is the most sensitive to changes in temperature. After optimization by B3LYP, D_1 isomer seemed to be the most stable one. The structure stability of D_1 and P_1 isomers in MD are similar. These two isomers are only slightly more sensitive to temperature as compared with the all-carbon C_{17}.

Other substructures/fragments related to the D_5 diamond (and its relative L5 lonsdaleite) were constructed and investigated for stability, by both static PM3 calculation and molecular dynamics simulation procedures as well. The results show a good stability of several hyper-rings made from the small fullerenes C_{20} and C_{28}, modulated function of the central hollow, and the type consisting of small cages. At normal temperature, the hexagonal hyper-rings are more stable (as given by PM3 data), while at higher temperature, the pentagonal ones appear more stable, at least as isolated fragments. The substructures belonging to D_5 and L_5 showed a pertinent stability, possibly increased in the infinite corresponding lattice. The actual study employed the molecular dynamics simulation in finding the temperature limits for the most important events in a molecule: changes in topology and next its destruction.

These results could be useful in guiding further reactions, e.g., the dimerization to C_{34} and condensation to adamantane-like structures, finally leading to the diamond D_5 or, in general, in the design and synthesis of new strong structures, with possible applications in nanotechnology.

References

Abell G (1985) Empirical chemical pseudopotential theory of molecular and metallic bonding. Phys Rev B 31:6184–6196

Aleksenskiĭ AE, Baĭdakova MV, Vul AY, Davydov VY, Pevtsova YA (1997) Diamond-graphite phase transition in ultradisperse-diamond clusters. Phys Solid State 39:1007–1015

Aste T, Weaire D (2008) The pursuit of perfect packing, 2nd edn. Taylor & Francis, London
Blasé X, Benedek G, Bernasconi M (2010) Structural, mechanical and supraconducting properties of clathrates. In: Colombo L, Fasolino A (eds) Computer-based modeling of novel carbon systems and their properties. Beyond nanotubes. Springer, Dordrecht, Chapter 6, pp 171–206
Brenner D (1990) Empirical potential for hydrocarbons for use in simulating the chemical vapor deposition of diamond films. Phys Rev B 42:9458–9471
Brenner D (1992) Empirical potential for hydrocarbons for use in simulating the chemical vapor deposition of diamond films. Phys Rev B 46:1948–1992
Brenner DW (2000) The art and science of an analytic potential. Phys Stat Sol 217:23–40
Brenner DW, Shenderova OA, Harrison JA, Stuart SJ, Ni B, Sinnott SB (2000) Second generation reactive empirical bond order (REBO) potential energy expression for hydrocarbons. J Phys Condens Matter 14:783–802
Case DA, Cheatham TE III, Darden T, Gohlke H, Luo R, Merz KM, Onufriev AJ, Simmerling C, Wang B, Woods R (2005) The Amber biomolecular simulation programs. J Comput Chem 26:1668–1688
Decarli PS, Jamieson JC (1961) Formation of diamond by explosive shock. Science 133: 1821–1822
Delgado-Friedrichs O, Foster MD, O'Keeffe M, Proserpio DM, Treacy MMJ, Yaghi OM (2005) What do we know about three-periodic nets? J Solid State Chem 178:2533–2554
Diudea MV (ed) (2005) Nanostructures, novel architecture. NOVA, New York
Diudea MV (2010a) Diamond D_5, a novel allotrope of carbon. Studia Univ Babes-Bolyai Chemia 55(4):11–17
Diudea MV (2010b) Nanomolecules and nanostructures – polynomials and indices. University of Kragujevac, Kragujevac
Diudea MV, Ilić A (2011) All-pentagonal face multi tori. J Comput Theor Nanosci 8:736–739
Diudea MV, Nagy CL (2007) Periodic nanostructures. Springer, Dordrecht
Diudea MV, Petitjean M (2008) Symmetry in multi tori. Symmetry Cult Sci 19(4):285–305
Diudea MV, Bende A, Janežič D (2010) Omega polynomial in diamond-like networks. Fuller Nanotub Carbon Nanostruct 18:236–243
Dubrovinskaia N, Dub S, Dubrovinsky L (2006) Superior wear resistance of aggregated diamond nanorods. Nano Lett 6:824–826
Eaton PE (1979) Towards dodecahedrane. Tetrahedron 35(19):2189–2223
Frondel C, Marvin UB (1967) Lonsdaleite a hexagonal polymorph of diamond. Nature 214: 587–589
Gaussian 09 (2009) Revision A.1, Frisch MJ, Trucks GW, Schlegel HB, Scuseria GE, Robb MA, Cheeseman JR, Scalmani G, Barone V, Mennucci B, Petersson GA, Nakatsuji H, Caricato M, Li X, Hratchian HP, Izmaylov AF, Bloino J, Zheng G, Sonnenberg JL, Hada M, Ehara M, Toyota K, Fukuda R, Hasegawa J, Ishida M, Nakajima T, Honda Y, Kitao O, Nakai H, Vreven T, Montgomery JA, Peralta JE, Ogliaro F, Bearpark M, Heyd JJ, Brothers E, Kudin KN, Staroverov VN, Kobayashi R, Normand J, Raghavachari K, Rendell A, Burant JC, Iyengar SS, Tomasi J, Cossi M, Rega N, Millam NJ, Klene M, Knox JE, Cross JB, Bakken V, Adamo C, Jaramillo J, Gomperts R, Stratmann RE, Yazyev O, Austin AJ, Cammi R, Pomelli C, Ochterski JW, Martin RL, Morokuma K, Zakrzewski VG, Voth GA, Salvador P, Dannenberg JJ, Dapprich S, Daniels AD, Farkas Ö, Foresman JB, Ortiz JV, Cioslowski J, Fox DJ, Gaussian Inc, Wallingford
Gestmann D, Kuck D, Pritzkow H (2006) Partially benzoannelated centro-hexaquinanes: oxidative degradation of centropolyindanes by using ruthenium (VIII) oxide and ozone. Liebigs Ann 1996:1349–1359
Gund P, Gund TM (1981) How many rings can share a quaternary atom? J Am Chem Soc 103:4458–4465
Hyde ST, Keeffe MO, Proserpio DM (2008) A short history of an elusive yet ubiquitous structure in chemistry, materials, and mathematics. Angew Chem Int Ed 47:7996–8000

Khachatryan AK, Aloyan SG, May PW, Sargsyan R, Khachatryan VA, Baghdasaryan VS (2008) Graphite-to-diamond transformation induced by ultrasound cavitation. Diam Relat Mater 17:931–936

Kuck D (1984) A facile route to benzoannelated centrotriquinanes. Angew Chem Int Ed 23: 508–509

Kuck D (2006) Three-dimensional hydrocarbon cores based on multiply fused cyclopentane and indane units: centropolyindanes. Chem Rev 106:4885–4925

Kuck D, Schuster A, Paisdor B, Gestmann D (1995) Benzoannelated centropolyquinanes. Part 21. Centrohexaindane: three complementary syntheses of the highest member of the centropolyindane family. J Chem Soc Perkin Trans 1 Org Bio-Org Chem 6:721–732

Kyani A, Diudea MV (2012) Molecular dynamics simulation study on the diamond D_5 substructures. Central Eur J Chem 10(4):1028–1033

Osawa E (2007) Recent progress and perspectives in single-digit nanodiamond. Diam Relat Mater 16:2018–2022

Osawa E (2008) Monodisperse single nanodiamond particulates. Pure Appl Chem 80:1365–1379

Paquette LA, Balogh DW, Usha R, Kountz D, Christoph GG (1981) Crystal and molecular structure of a pentagonal dodecahedrane. Science 211:575–576

Paquette LA, Vazeux M (1981) Threefold transannular epoxide cyclization: synthesis of a heterocyclic C_{17}-hexaquinane. Tetrahedron Lett 22:291–294

Plimpton SJ (1995) Fast parallel algorithms for short-range molecular dynamics. Comp Phys 117:1–19

Prinzbach H, Wahl F, Weiler A, Landenberger P, Wörth J, Scott LT, Gelmont M, Olevano D, Sommer F, Bv I (2006) C_{20} carbon clusters: fullerene-boat-sheet generation, mass selection, photoelectron characterization. Chem Eur J 12:6268–6280

Rafii-Tabar H (2004) Computational modelling of the thermo-mechanical and transport properties of carbon nanotubes. Phys Rep 390:235–452

Ruoff R, Qian D, Liu W (2003) Mechanical properties of carbon nanotubes: theoretical predictions and experimental measurements. C R Phys 4:993–1008

Saito M, Miyamoto Y (2001) Theoretical identification of the smallest fullerene, C_{20}. Phys Rev Lett 87:035503

Simmons HE III, Maggio JE (1981) Synthesis of the first topologically non-planar molecule. Tetrahedron Lett 22:287–290

Stuart SJ, Tutein AB, Harrison JA (2000) A reactive potential for hydrocarbons with intermolecular interactions. J Chem Phys 112:6472–6486

Szefler B, Diudea MV (2012) On molecular dynamics of the diamond D5 seeds. Struct Chem 23(3):717–722

Tersoff J (1988a) New empirical approach for the structure and energy of covalent systems. Phys Rev B 37:6991–7000

Tersoff J (1988b) Empirical interatomic potential for carbon, with applications to amorphous carbon. Phys Rev Lett 61:2879–2882

Verlet L (1967) Computer "experiments" on classical fluids. I. Thermodynamical properties of Lennard-Jones molecules. Phys Rev 159:98–103

Verlet L (1968) Computer "experiments" on classical fluids II. Equilibrium correlation functions. Phys Rev 165:201–214

Wang J, Cieplak P, Kollman PA (2000) How well does a restrained electrostatic potential (RESP) model perform in calculating conformational energies of organic and biological molecules? J Comput Chem 21:1049–1074

Wang J, Wolf RM, Caldwell JW, Kollamn PA, Case DA (2004) Development and testing of a general amber force field. J Comput Chem 25:1157–1174

Williams OA, Douhéret O, Daenen M, Haenen K, Osawa E, Takahashi M (2007) Enhanced diamond nucleation on monodispersed nanocrystalline diamond. Chem Phys Lett 445:255–258